Attractors near grazing-sliding bifurcations

Glendinning, Paul and Kowalczyk, Piotr and Nordmark, Arne

2011

MIMS EPrint: **2011.63**

ISSN 1749-9097

Attractors near grazing-sliding bifurcations

P. Glendinning [*], Piotr Kowalczyk [†] and A. B. Nordmark [‡]

April 6, 2011

Abstract

In this paper we prove, for the first time, that multistability can occur in 3-dimensional Fillipov type flows due to grazing-sliding bifurcations. We do this by reducing the study of the dynamics of Filippov type flows around a grazing-sliding bifurcation to the study of appropriately defined one-dimensional maps. In particular, we prove the presence of three qualitatively different types of multiple attractors born in grazing-sliding bifurcations. Namely, a period-two orbit with a sliding segment may coexsist with a chaotic attractor, two stable, period-two and period-three orbits with a segment of sliding each may coexist, or a non-sliding and period-three orbit with two sliding segments may coexist.

Keywords: Multiple attractors, grazing-sliding bifurcations, one-dimensional maps;
PACS numbers: 05.45.Ac, 05.45 -a, 02.30.Oz;

1 Introduction

Many systems of relevance to applications are modelled as switched systems. Consider a simple bang-bang feedback control which is a common strategy in control engineering [1, 2]; the control is switched on or off when the output crosses certain threshold value or alternatively a switch between different system configurations may occur. Another example can be given from the area of mechanical engineering and robotics. The occurrence of 'stiction' (static forces) implies that, for instance, a slowly moving activated arm of a robot may exhibit 'jitters' due to the presence of stick-slip motion of mechanical elements. Auto-adhesion or stiction is also an important reliability issue in micro-electromechanical systems [3]. In the mechanical examples given the presence of 'stiction' implies switching between the dynamics with the kinematic friction force, and the dynamics characterised by the static friction force.

The presence of switchings is limited not only to engineering systems, but is also present in living organisms. Genetic regulatory networks work on the on/off activation/inhibition principle [4]. Taking into account the aforementioned examples it is not surprising that scientists turned their attention to study the dynamics of switched or piecewise-smooth systems. The presence of switchings translates in the mathematical model to the presence of sets (or manifolds), often termed as switching manifolds or discontinuity sets, on which vector fields that model a particular physical

[*]Centre for Interdisciplinary Computational and Dynamical Analysis (CICADA) and School of Mathematics, The University of Manchester, Oxford Road, Manchester M13 9PL, U.K., Email: p.a.glendinning@manchester.ac.uk
[†]*Corresponding Author.* School of Computing, Mathematics and Digital Technology, John Dalton Building, Manchester Metropolitan University, Chester Street, Manchester, M1 5GD, U.K., Email: p.kowalczyk@mmu.ac.uk
[‡]Department of Mechanics, KTH, 100 44 Stockholm, Sweden, Email: nordmark@mech.kth.se

system lose their smoothness properties. When the vector field that governs system dynamics is discontinuous across the switching manifold such systems are termed as *Filippov* type systems. A particular feature of Filippov systems is so-called *sliding motion* which is a motion within the system's discontinuity set.

There is ample literature where different aspects of the dynamics triggered by the presence of discontinuous nonlinearities have been treated, and in particular, bifurcations induced by the presence of discontinuity sets (Discontinuity Induced Bifurcations or DIBs for short) have been given much focus, see for example [5, 6, 7, 8, 9, 10, 11, 12, 13, 14]. However, there is a number of important and intriguing questions that have not been answered as yet. One of the open problems is whether multiple attractors can be born in the grazing-sliding bifurcations in three-dimensional Filippov type flows, and if this is the case, what is the mechanism leading to their birth. So far, the reported occurrence of multiple attractors born in the DIBs have been limited to switched systems where sliding is not possible, see for example [15]. Multiple attractors have been also observed in two-dimensional piecewise-affine maps where their birth is linked with the occurrence of border-collision bifurcations [8]. In the current paper, for the first time we prove that, indeed, grazing-sliding bifurcations in three-dimensional Filippov type flows may lead to the birth of multiple attractors. This is shown by reducing a generic three-dimensional Filippov type flow about a grazing-sliding bifurcation to appropriately defined one-dimensional maps. We then show that three different types of multistability can occur in these maps.

The rest of the paper is outlined as follows. In Sec. 2 we introduce the phase space topology of Filippov systems. The analytical conditions for a grazing-sliding bifurcation as well as the the normal form map for this bifurcation are then given. In Sec. 3 the reduction to one-dimensional maps allows us to show that three distinct cases of multistability in the grazing-sliding bifurcation occur. Analytical proofs for multistability are given in Sec. 4 together with numerically computed examples.

2 Grazing-sliding; canonical form for $3-$dimensional Filippov type flows

2.1 Phase space topology

Consider Filippov systems for which the evolution of variable $\mathbf{x}$ in some region $D \subseteq \mathbb{R}^3$ is determined by the equations

$$\dot{\mathbf{x}}(t) = \begin{cases} F_1(\mathbf{x}(t), \mu) & \text{if} \quad H(\mathbf{x}(t), \mu) > 0 \\ F_2(\mathbf{x}(t), \mu) & \text{if} \quad H(\mathbf{x}(t), \mu) < 0, \end{cases} \tag{1}$$

where $F_1,\ F_2$ are sufficiently smooth vector functions, $F_1,\ F_2 : \mathbb{R}^3 \times \mathbb{R} \mapsto \mathbb{R}^3$, and $H(\mathbf{x}(t), \mu) : \mathbb{R}^3 \times \mathbb{R} \mapsto \mathbb{R}$ is some smooth scalar function depending on system states $\mathbf{x} \in \mathbb{R}^3$, and parameter $\mu \in \mathbb{R}$; $t \in \mathbb{R}$ is the time variable. Let us define the boundary Σ as

$$\Sigma := \{\mathbf{x} \in \mathbb{R}^3 : H(\mathbf{x}(t), \mu) = 0\} \tag{2}$$

which divides region D into two subspaces:

$$G_1 := \{\mathbf{x} \in \mathbb{R}^3 : H(\mathbf{x},\, \mu) > 0\},$$

and

$$G_2 := \{\mathbf{x} \in \mathbb{R}^3 : H(\mathbf{x},\, \mu) < 0\},$$

in which the dynamics is smooth. Depending on the direction of the vector fields with respect to Σ those trajectories starting in G_1 and G_2 that reach Σ in finite time will either cross or evolve along Σ (the so-called sliding motion). Let $\sigma(\mathbf{x}) = \langle H_x, F_1\rangle\langle H_x, F_2\rangle$, where $\langle,\rangle$ denotes the dot product and H_x is the vector normal to Σ. The switching surface Σ can be divided into subsets, say Σ_c and $\hat{\Sigma}$, defined as

$$\Sigma_c := \{\mathbf{x} \in \Sigma : \sigma(\mathbf{x}) > 0\}, \qquad \hat{\Sigma} := \{\mathbf{x} \in \Sigma : \sigma(\mathbf{x}) \leq 0\}.$$

When a trajectory generated by F_1 (or F_2) reaches Σ_c it switches to F_2 (or F_1) on Σ_c. Note that such a trajectory is continuous, and it is built of segments generated by F_1 and F_2. If, on the other hand, $\hat{\Sigma}$ is reached from G_1 or G_2, then the motion follows so called sliding flow along $\hat{\Sigma}$, and the vector field that generates this motion is defined as

$$F_s = \alpha_s F_1 + (1 - \alpha_s)F_2, \tag{3}$$

where $\alpha_s = \alpha_s(\mathbf{x}) = \dfrac{\langle H_x, F_2\rangle}{\langle H_x, (F_2 - F_1)\rangle}$, and $0 \leq \alpha_s(\mathbf{x}) \leq 1$. The function $\alpha(\mathbf{x})$ can be used to define the boundaries of a region where sliding is possible, namely

$$\partial\hat{\Sigma} := \{\mathbf{x} \in \Sigma : \alpha_s = 1\}, \qquad \partial\hat{\Sigma}^0 := \{\mathbf{x} \in \Sigma : \alpha_s = 0\}.$$

The condition for the existence of an *attracting* sliding region within Σ is that the vector fields point toward Σ from either sides of the switching surface, that is

$$\langle H_x, F_2\rangle > 0, \quad and \quad \langle H_x, F_1\rangle < 0,$$

within $\hat{\Sigma}$, and with $\langle H_x, F_2\rangle = 0$ on $\partial\hat{\Sigma}^0$ and $\langle H_x, F_1\rangle = 0$ on $\partial\hat{\Sigma}$; thus on the boundary $\partial\hat{\Sigma}$

$$\langle H_x, (F_2^* - F_1^*)\rangle > 0. \tag{4}$$

Assume that an isolated periodic orbit exists in G_1, and so it is solely generated by F_1. Furthermore assume that at $\mu = 0$ this periodic orbit undergoes a grazing-sliding bifurcation. The assumption that grazing occurs at the particular value of $\mu = 0$ can be introduced without the loss of generality since a translation ensures this. In this setting there exists a point $\mathbf{x}^*$ on the limit cycle that at $\mu = 0$ exhibits a grazing contact with the boundary $\partial\hat{\Sigma}$, and under the variation of μ through 0 there exists at least one limit cycle with a short segment of sliding [16].

We choose $(x,\, y,\, z)$ coordinates such that the Poincaré section Π, transversal to the flow generated by the vector field F_1 and containing $\mathbf{x}^*$, is given by $\Pi := \{(x,\, z) \in \mathbb{R}^2,\, y = \langle H_x, F_1\rangle = 0\}$. In the chosen coordinate set assume that $H(\mathbf{x},\, \mu)$ is independent of μ and z. Finally, since we are interested in the dynamics locally about $\mathbf{x}^*$, we assume that H is linear in x, and we introduce a coordinate shift so that the grazing point of the cycle is located at $\mathbf{x}^* = 0$. The choice of the Poincaré section implies that trajectories generated by F_1, locally around the grazing point, reach their minimum with respect to Σ on Π.

2.2 Analytical conditions and Poincaré return map

At $\mathbf{x}^* = (0,\, 0,\, 0)$ the following defining conditions for a grazing-sliding bifurcation must hold

$$H(\mathbf{x}^*) = x^* = 0, \tag{5}$$

$$\langle H_x, F_1(\mathbf{x}^*,\, 0)\rangle = 0, \tag{6}$$

and the non-degeneracy condition

$$\langle (H_x F_1)_x, F_1(\mathbf{x}^*,\, 0)\rangle > 0.$$

Let P be the first return map from the chosen Poincaré section Π that maps points from a sufficiently small neighbourhood of $\mathbf{x}^*$ back to itself ignoring the presence of switching. The existence of diffeomorphism P (locally about x^*) is guaranteed by the existence of an isolated periodic orbit and the differentiability of F_1. Assume now that the parameter μ unfolds the bifurcation; so

$$\left.\frac{\partial P^x}{\partial \mu}\right|_{(x^*,0)} \neq 0,$$

where superscript 'x' denotes the component of the map along the x-axis.

To obtain a map that maps points from a sufficiently small neighbourhood of $\mathbf{x}^*$ back to itself, taking into account the presence of switching (and the sliding flow), we have to compose the piecewise affine approximation of the map P with so-called Poincaré Discontinuity Map (PDM) which take trajectories which strike the Poincaré section in $H(x, 0, z) \leq 0$ backwards in time to where it would have intersected the switching surface and then forwards in time to where the sliding orbit exists the switching surface. As shown in [14] this map can be written to lowest order as

$$PDM(x, z) = \begin{cases} \mathbf{x} & \text{for } H(x,\, 0,\, z) > 0 \\ \mathbf{x} - H(x,\, 0,\, z)\left(\dfrac{F_2(\mathbf{x}^*)}{\langle H_x, (F_2(\mathbf{x}^*) - F_1(\mathbf{x}^*))\rangle} + KF_1(\mathbf{x}^*)\right) & \text{for } H(x,\, 0,\, z) \leq 0, \end{cases} \tag{7}$$

where

$$K = \frac{\langle (H_x F_1(x^*))_x, F_2(x^*)\rangle}{\langle (H_x F_1(x^*))_x, F_1(x^*)\rangle}$$

is some non-zero constant depending on the vector fields F_1 and F_2, its Jacobians, on the vector normal to Σ (H_x), and the Hessian matrix, say H_{xx}. Subscript 'x' denotes the operation of differentiation and repeated usage of 'x' refers to the repeated action of differentiation.

In our case the PDM simplifies to

$$PDM(x, z) = \begin{cases} \mathbf{x} & \text{for } x > 0 \\ \mathbf{x} - x\left([1,\, a]^T + [0,\, K']^T\right) & \text{for } x \leq 0, \end{cases} \tag{8}$$

where

$$a = \frac{F_2^z(x^*)}{F_2^x(x^*)},$$

and

$$K' = KF_1^z(x^*) = \frac{f_{11}F_2^x + f_{12}F_2^z}{f_{12}} = \frac{f_{11}F_2^x}{f_{12}} + F_2^z;$$

superscripts denote the components of the vector field F_2 in the direction labelled, and f_{1i}, with $i = 1,\, 2$, are the first row components of the jacobian matrix of the vector field F_1 calculated at the grazing point.

Using the defining condition (6) for a grazing-sliding bifurcation we note that the first component of the vector field F_1 at the grazing point $\mathbf{x}^*$ is 0, and $F_2^x > 0$ by (4). It then follows that (8) can be simplified to yield

$$PDM(x, z) = \begin{cases} \mathbf{x} & \text{for } x > 0 \\ \begin{pmatrix} 0 \\ \bar{C}x + z \end{pmatrix} & \text{for } x \leq 0, \end{cases} \tag{9}$$

where $\bar{C} = -(a + K')$ can be an arbitrary constant because there are no restrictions on f_{11}, f_{12}, and F_2^z. Equivalently we have

$$PDM(x, z) = \begin{cases} \begin{pmatrix} x \\ z \end{pmatrix} & \text{for } x > 0 \\ A_s \mathbf{x} & \text{for } x \leq 0, \end{cases} \tag{10}$$

where

$$A_s = \begin{pmatrix} 0 & 0 \\ \bar{C} & 1 \end{pmatrix}.$$

The piecewise affine approximation of the map P, say P_A, can be given by

$$P_A(x,\, z;\, \bar{\mu}) = \begin{pmatrix} a_{11} & a_{12} \\ a_{21} & a_{22} \end{pmatrix} \begin{pmatrix} x \\ z \end{pmatrix} + \bar{\mu} \begin{pmatrix} b_1 \\ b_2 \end{pmatrix}, \tag{11}$$

where a_{11}, a_{12}, a_{21}, a_{22}, $b_1 \neq 0$, b_2 are arbitrary, but fixed, constants and such that the matrix

$$\bar{A} = \begin{pmatrix} a_{11} & a_{12} \\ a_{21} & a_{22} \end{pmatrix}$$

is full rank and has no eigenvalues on the unit circle of the complex plane, which is equivalent to saying that the grazing orbit is unique; the requirement on b_1 being non-zero is equivalent to requiring $\bar{\mu}$ being the unfolding parameter.

2.3 Coordinate transformation

Assume $a_{12} \neq 0$ and let $[u,\, v']^T = L[x,\, z]^T$, where

$$L = \begin{pmatrix} 1 & 0 \\ -a_{22} & a_{12} \end{pmatrix}, \tag{12}$$

and

$$L^{-1} = \begin{pmatrix} 1 & 0 \\ a_{22}/a_{12} & 1/a_{12} \end{pmatrix}. \tag{13}$$

Then the affine map P_A becomes

$$\begin{pmatrix} u \\ v' \end{pmatrix} \mapsto L\bar{A}L^{-1} \begin{pmatrix} u \\ v' \end{pmatrix} = \begin{pmatrix} T & 1 \\ -D & 0 \end{pmatrix} \begin{pmatrix} u \\ v' \end{pmatrix} + \mathbf{b}'\bar{\mu}, \tag{14}$$

where $T = a_{11} + a_{22}$ is the trace and $D = a_{11}a_{22} - a_{12}a_{21}$ is the determinant of the matrix $\bar{A}$, and

$$\mathbf{b}' = \begin{pmatrix} b_1 \\ -a_{22}b_1 + a_{12}b_2 \end{pmatrix}.$$

The discontinuity map PDM becomes

$$\begin{pmatrix} u \\ v' \end{pmatrix} \mapsto LA_sL^{-1} \begin{pmatrix} u \\ v' \end{pmatrix} = \begin{pmatrix} 0 & 0 \\ C & 1 \end{pmatrix} \begin{pmatrix} u \\ v' \end{pmatrix}, \tag{15}$$

where $C = a_{22} + \bar{C}a_{12}$. Let $v = v' + (a_{22}b_1 - a_{12}b_2)\bar{\mu}$. Then for the affine map we have

$$\begin{pmatrix} u \\ v \end{pmatrix} \mapsto \begin{pmatrix} T & 1 \\ -D & 0 \end{pmatrix} \begin{pmatrix} u \\ v \end{pmatrix} + \begin{pmatrix} (1 - a_{22})b_1 + a_{12}b_2 \\ 0 \end{pmatrix} \bar{\mu}$$

with PDM changing the coordinates to $(u,\, v)$, but otherwise left unaltered. Finally by scaling $\bar{\mu}((1-a_{22})b_1 + a_{12}b_2) = \mu$ we obtain

$$P_A(u,\, v;\, \mu) = \begin{pmatrix} T & 1 \\ -D & 0 \end{pmatrix} \begin{pmatrix} u \\ v \end{pmatrix} + \mu \begin{pmatrix} 1 \\ 0 \end{pmatrix}, \tag{16}$$

$$PDM(u,\, v;\, \mu) = \begin{pmatrix} 0 & 0 \\ C & 1 \end{pmatrix} \begin{pmatrix} u \\ v \end{pmatrix}. \tag{17}$$

It is the form (16) and (17) that we use in the subsequent analysis. However, different forms of the maps may be considered for the analytical and numerical purposes (see the Appendix).

3 One-dimensional maps

For the sake of clarity in the remaining part of the paper we use the following representation for the affine map (16) and for PDM:

$$P_A\left(x, \quad z; \quad \mu\right) = A\begin{pmatrix} x \\ z \end{pmatrix} + \mathbf{b}\mu \tag{18}$$

where

$$A = \begin{pmatrix} a & 1 \\ -b & 0 \end{pmatrix}, \qquad \mathbf{b} = \begin{pmatrix} 1 \\ 0 \end{pmatrix},$$

and

$$PDM\left(x, \quad z; \quad \mu\right) = \begin{pmatrix} 0 & 0 \\ C & 1 \end{pmatrix} \begin{pmatrix} x \\ z \end{pmatrix} \tag{19}$$

with PDM being the identity for $x > 0$. The approach taken by [14] and others has been to say that if we have a point (x, z) on the return plane with $x < 0$ then we use PDM to determine where it would have struck and then P_A to bring it back to the return plane, i.e. the return map if $x < 0$ is $P_A \circ PDM$, or

$$\begin{pmatrix} x' \\ z' \end{pmatrix} = P_A \circ PDM(x, z) = \begin{pmatrix} 0 \\ z \end{pmatrix}. \tag{20}$$

Whilst this is perfectly correct, we choose to emphasise the one-dimensional nature of the return map by not applying P_A at this stage. Thus any solution of (1) which intersects the switching surface at some stage is mapped to $x = 0$ on the return plane, and then either stays in $x > 0$ or returns to $\{y = 0\}$ with $x < 0$, where it is mapped to $x = 0$ by PDM. We will choose to look for returns to the line $x = 0$ on the return plane, thus constructing a one dimensional map in the $z-$coordinate:

$$z_{n+1} = f(z_n), \tag{21}$$

where f is piecewise affine. We now will start to determine f and some of its properties.

Suppose a solution starts on the return plane at (x_0, z_0) with $x_0 \geq 0$. The first return is given by the map P_A defined by

$$\begin{pmatrix} x_{n+1} \\ z_{n+1} \end{pmatrix} = \begin{pmatrix} a & 1 \\ -b & 0 \end{pmatrix} \begin{pmatrix} x_n \\ z_n \end{pmatrix} + \mu \begin{pmatrix} 1 \\ 0 \end{pmatrix}, \tag{22}$$

and whilst $x_k \geq 0$, $k = 1, 2, \ldots n$, this map continues to define the next return of a solution. Now, the n^{th} iterate of an affine map $\mathbf{x} \to A\mathbf{x} + \mathbf{b}$ is

$$\mathbf{x} \to A^n\mathbf{x} + (A^{n-1} + A^{n-2} + \cdots + I)\mathbf{b},$$

and so we are able to write higher iterates of the map in terms of the entries of powers of the matrix A. Using the notation $(A^n)_{ij} = a_{ij}^{(n)}$ a straightforward exercise in linear algebra shows that provided $x_k > 0$, $k = 0, \ldots, n-1$, then the image of a point on the intersection of the sliding surface with the return plane, $(0, z)^T$, under n iterations of (22) is

$$\begin{pmatrix} x_n \\ z_n \end{pmatrix} = \begin{pmatrix} a_{12}^{(n)} z + (\sum_{k=1}^{n-1} a_{11}^{(k)} + 1)\mu \\ a_{22}^{(n)} z + (\sum_{k=1}^{n-1} a_{21}^{(k)})\mu \end{pmatrix}. \tag{23}$$

If $x_n < 0$ then this is not actually the point of intersection of the solution; it will have struck the sliding surface on that last circuit in $x > 0$ and the PDM is needed to find the true point of intersection, which will be on the $z-$axis again, at $(0, z')$ where

$$z' = C\left(a_{12}^{(n)} z + (\sum_{k=1}^{n-1} a_{11}^{(k)} + 1)\mu\right) + a_{22}^{(n)} z + (\sum_{k=1}^{n-1} a_{21}^{(k)})\mu. \tag{24}$$

Thus the return map f of (21) can be written in terms of a countable set of affine maps f_i with (possibly empty) domains D_i:

$$f_i(z) = (Ca_{12}^{(n)} + a_{22}^{(n)})z + \left(C + \sum_{k=1}^{n-1}(Ca_{11}^{(k)} + a_{21}^{(k)})\right)\mu, \tag{25}$$

and the domain on which this is applied is D_i defined as the set of z such that

$$a_{12}^{(m)} z + (\sum_{k=1}^{m-1} a_{11}^{(k)} + 1)\mu \geq 0, \;\; m = 1, \ldots, n-1, \tag{26}$$

and

$$a_{12}^{(n)} z + (\sum_{k=1}^{n-1} a_{11}^{(k)} + 1)\mu < 0. \tag{27}$$

In terms of these maps (21) becomes

$$z_{n+1} = f_i(z_n) \;\; \text{if} \;\; z_n \in D_i. \tag{28}$$

As already suggested, the crucial consideration when applying these maps is to determine how many of the sets D_i are non-empty. Note that if $z \notin D_i$ for all i then the solution through $(0, z)^T$ on the return plane never has a non-trivial sliding section in future time.

The remainder of this paper is devoted to analyzing different cases of these maps. We begin with some obvious statements about f_1.

If $z + \mu < 0$ we apply PDM, given by (19), to bring us back to the correct location on the return plane with $x = 0$ after one passage in $x > 0$ and a sliding section giving the return map f_1:

$$z \to C(z + \mu).$$

or

$$z_{n+1} = f_1(z_n) = C(z + \mu), \qquad \text{for} \qquad z + \mu < 0. \tag{29}$$

This already permits us to determine the existence and stability properties of periodic orbits with one sliding section, as these are fixed points of f_1.

Using elementary calculations it can be easily shown that if $\mu > 0$ then a periodic point corresponding to the sliding orbit exists for $C > 1$, and hence it is unstable. On the other hand for μ negative $C \in (-\infty,\ 1)$ and the sliding orbit can be either stable, for $C \in (-1,\ 1)$, or unstable, for $C \in (-\infty,\ -1)$.

For the sake of completeness we determine the condition for the existence of the fixed point corresponding to the non-sliding cycle, which is a fixed point of the affine map (18). Call this fixed point $X^*(x^*, z^*)$. We then have $X^* = \left(\frac{\mu}{1-a+b},\ -\frac{b\mu}{1-a+b}\right)$ and it exists iff $\frac{(1-a)\mu}{1-a+b} > 0$.

4 Multiple attractors

Figure 1 shows the results of iterating the return map (21) at two different parameter values. In Fig. 1(a), for $a = 0.05$, $b = 0.31$ and $\gamma = -C = 3$, two stable fixed points coexist: one corresponding to a slide following two circuits around the periodic orbit of the flow (see the middle branch), and the other corresponding to a slide following three circuits close to the periodic orbit (see the rightmost branch). The fixed point in the leftmost branch corresponds to an unstable periodic orbit with one sliding segment. In Fig. 2 we show bifurcation diagrams depicting these stable attractors with sliding segments bifurcating into a stable non-sliding orbit (parameter values are as in Fig. 1(a)). Namely, in Fig. 2(a) a stable period-two orbit with a segment of sliding (see the corresponding fixed point in the middle branch in Figure 1(a)), existing for $\mu < 0$, bifurcates into a non-sliding attractor, existing for $\mu > 0$. In Fig. 2(b) we can see a stable period-three orbit with a segment of sliding (see the corresponding fixed point in the rightmost branch in Figure 1(a)), existing for $\mu < 0$, bifurcating into the same non-sliding attractor as before.

In Fig. 1(b), for $a = 0.35$, $b = 0.3$ and $\gamma = -C = 3$, the coexistence of a chaotic attractor (involving one circuit and two circuit segments separated by sliding) and a stable fixed point (three circuits and one slide) is visible. As in the previous case we show bifurcation diagrams depicting these attractors bifurcating into a stable non-sliding orbit (parameter values are as in Fig. 1(b)). Namely, in Fig. 3(a) a bifurcation between a chaotic attractor, existing for $\mu < 0$, and a stable periodic orbit, existing for $\mu > 0$, is depicted. In Fig. 3(b) we can see a stable period-three orbit with a segment of sliding, existing for $\mu < 0$, bifurcating into the same stable non-sliding orbit.

In both cases of the multistability described above the return map has three monotonic branches, and the aim of this section is to prove the existence of regions in parameter space for which these phenomena can occur. Using (18) to calculate the return map on $x = 0$ we see that after one circuit a point $(0, z)$ is mapped to $(z + \mu, 0)$ and so it is followed by sliding if $z + \mu < 0$ with the PDM mapping to $(0, z')$ where

$$z' = C(z + \mu). \tag{30}$$

If $z + \mu > 0$ then a second application of the affine return map gives $(a(z + \mu) + \mu, -b(z + \mu))$ and so the PDM can be applied if $a(z + \mu) + \mu < 0$, mapping to $(0, z')$ where

$$z' = C(a(z + \mu) + \mu) - b(z + \mu). \tag{31}$$

Finally, if $z + \mu > 0$ and $a(z + \mu) + \mu > 0$ then a third application of the linear map gives

$$((a^2 - b)(z + \mu) + (a + 1)\mu, -b(a(z + \mu) + \mu))$$

and so if $((a^2 - b)(z + \mu) + (a + 1)\mu < 0$ the PDM gives the image $(0, z')$ where

$$z' = C((a^2 - b)(z + \mu) + (a + 1)\mu) - b(a(z + \mu) + \mu). \tag{32}$$

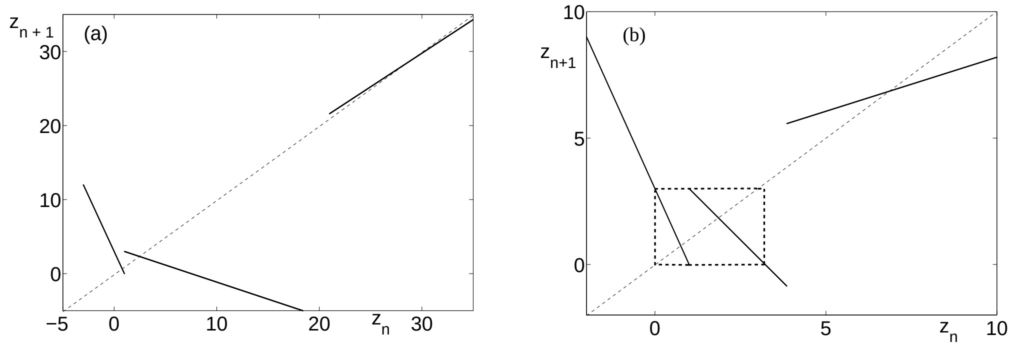

Figure 1: Graphs of the return map (21). In (a) we observe the coexistence of two stable fixed points for $\mu = -1$, $a = 0.05$, $b = 0.31$ and $\gamma = -C = 3$. In (b) we observe the coexistence of: a fixed point and a chaotic attractor (in box), for $a = 0.35$, $b = 0.3$ and $\gamma = -C = 3$.

The region of parameter values we have analyzed which allow for multistability have $\mu < 0$ (so we can take $\mu = -1$ by rescaling), with $a > 0$, $b > a^2$ and $C < 0$. The expressions are further simplified by writing them in terms of a new variable $w = z + \mu$. In these co-ordinates, and with the restrictions

$$\mu = -1, \quad a > 0, \quad b > a^2, \quad \gamma = -C > 0 \tag{33}$$

the maps (30-32) become

$$w_{n+1} = \begin{cases} -\gamma w_n - 1 & \text{if } w_n < 0 \\ -(\gamma a + b)w_n + \gamma - 1 & \text{if } 0 < w_n < 1/a \\ (\gamma(b - a^2) - ab)w_n + \gamma(a+1) + b - 1 & \text{if } w_n > 1/a. \end{cases} \tag{34}$$

In this section we will prove

Theorem 1 *Consider the map (34) subject to the constraints (33). For each* (a, γ) *with*

$$\gamma > 1, \quad a < 1, \quad 0 < a < \frac{\gamma - 1}{\gamma^2 - \gamma + 1}$$

there is a non-trivial interval of $b-$*values such that the map has two stable fixed points, one in* $(0, 1/a)$ *and the other in* $(1/a, \infty)$*. For each* (a, γ) *with*

$$\gamma > 1, \quad \frac{\gamma - 1}{\gamma^2 + 1} < a < \frac{\gamma - 1}{\gamma^2 - \gamma + 1}$$

there is a non-trivial interval of $b-$*values such that the map has a chaotic attractor in* $[-1, \gamma - 1]$ *and a stable fixed point in* $(1/a, \infty)$*.*

The conditions for the coexistence of fixed points is optimal, and we will determine the interval of $b-$values explicitly, but the condition on the coexistence of the fixed point and chaotic attractor has been chosen for simplicity; other values may be possible. The next two subsections prove the two statements separately.

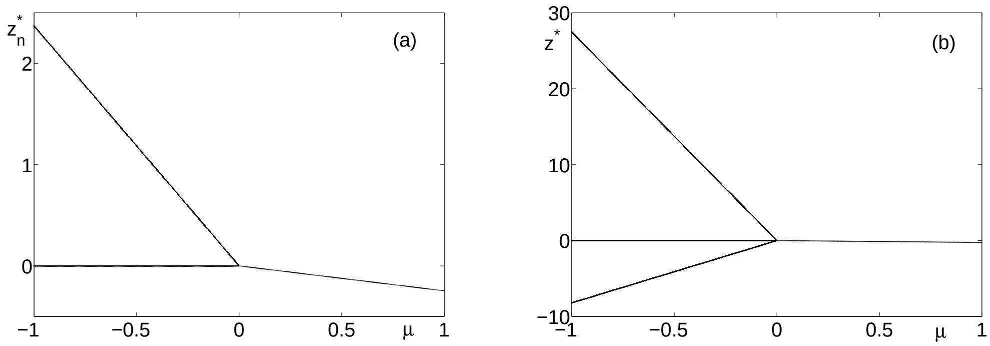

Figure 2: One-parameter bifurcation diagrams in μ for $a = 0.05$, $b = 0.31$ and $\gamma = -C = 3$ depicting (a) a period-two orbit coexisting with (b) a period-three orbit. The two stable orbits coexist for $\mu < 0$ and bifurcate into a periodic orbit when $\mu > 0$.

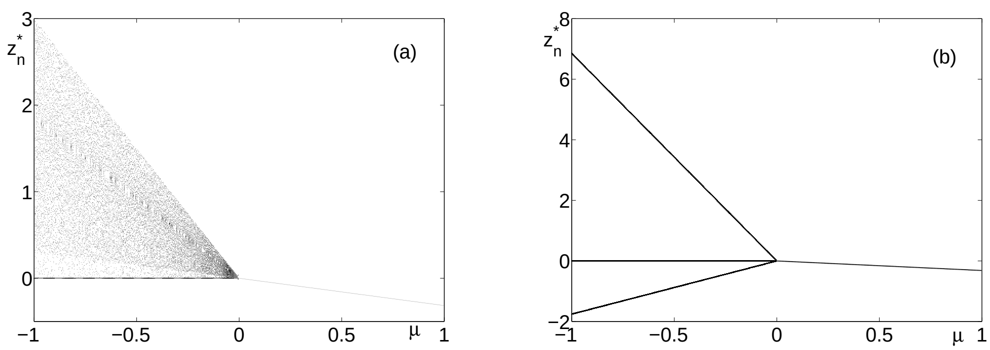

Figure 3: One-parameter bifurcation diagrams in μ for $a = 0.35$, $b = 0.3$ and $\gamma = -C = 3$. In (a) we depict a chaotic attractor coexisting with (b) a stable period-three orbit. Both stable orbits exist for $\mu < 0$ and bifurcate into a stable periodic orbit existing for $\mu > 0$.

4.1 Coexisting stable fixed points

To prove Theorem 1 let us first determine the conditions for a stable fixed point to exist in $(0, 1/a)$ and independently that a stable fixed point exists in $w > 1/a$.

The solution to the fixed point equation in $(0, 1/a)$ is

$$w_2 = \frac{\gamma - 1}{\gamma a + b + 1},$$

and this is valid if it lies in the interval $(0, 1/a)$. Clearly $w_2 > 0$ provided $\gamma > 1$ as γ, a and b are all positive by (33). Incidently, this shows that w_2 cannot coexist with a stable fixed point in $x < 0$. Similarly, $w_2 < 1/a$ provided $a(\gamma-1) < \gamma a + b + 1$ or $0 < a + b + 1$, which is not a further restriction of the conditions we have obtained. Finally, w_2 is stable if it exists and $|\gamma a + b| < 1$, and (as the parameters are all positive) we can omit the modulus sign. There is a stable fixed point in $(0, 1/a)$ iff (33) holds and

$$\gamma > 1, \quad \gamma a + b < 1. \tag{35}$$

We now repeat these elementary considerations for fixed points in $w > 1/a$. The fixed point equation gives

$$w_3 = \frac{\gamma(a+1) + b - 1}{1 + ab - \gamma(b - a^2)},$$

and so there is a stable fixed point if $w_3 > 1/a$ and $|\gamma(b - a^2) - ab| < 1$. The second of these conditions can be written as

$$-1 < \gamma(b - a^2) - ab < 1 \tag{36}$$

which implies that the denominator of the expression for w_3 is positive, and if the numerator is also positive,

$$\gamma(a+1) + b - 1 > 0 \tag{37}$$

and then the condition $w_3 > 1/a$ is

$$\frac{a+1}{\gamma} - a < b. \tag{38}$$

Inequalities (36), (37) and (38) together with (33) give the general conditions for a stable fixed point in $w > 1/a$ which will be required later, but they simplify if the extra constraints (35) for the existence of a stable fixed point in $(0, 1/a)$ are included.

In this multistable case, $\gamma a + b < 1$ and $\gamma > 1$ implies that (37) is automatically satisfied and we need only consider (36) and (38). Rewriting (38) as

$$-1 + \gamma a^2 < b(\gamma - a) < 1 + \gamma a^2$$

and since $\gamma > 1$ and $b < 1 - \gamma a$ from (35), $\gamma > 1 > a$ so we can collect together all the inequalities involving b in the form

$$s < b < S \tag{39}$$

where

$$s = \max\left(\frac{-1 + \gamma a^2}{\gamma - a}, a^2, \frac{a+1}{\gamma} - a\right), \tag{40}$$

and

$$S = \min\left(\frac{1 + \gamma a^2}{\gamma - a}, 1 - \gamma a\right). \tag{41}$$

Now, a tiresome but straightforward calculation shows that $\dfrac{-1+\gamma a^2}{\gamma - a} < a^2$ as $0 < a < 1$, and $a^2 < \dfrac{a+1}{\gamma} - a$ as $\gamma a < 1$, hence $s < S$ and there is an interval of $b-$values defined by (39) if

$$\frac{a+1}{\gamma} - a < \min\left(\frac{1+\gamma a^2}{\gamma - a}, 1 - \gamma a\right).$$

Another routine calculation shows that $\dfrac{a+1}{\gamma} - a < \dfrac{1+\gamma a^2}{\gamma - a}$ as $\gamma > 1$ leaving only one active condition: $\dfrac{a+1}{\gamma} - a < 1 - \gamma a$ which, after some more manipulation is equivalent to

$$a < \frac{\gamma - 1}{\gamma^2 - \gamma + 1}$$

as stated in the Theorem.

4.2 Coexisting stable fixed point and chaotic attractor

For the second part of the theorem, the coexistence of a chaotic attractor with a stable fixed point, we keep conditions (33), with (36), (37) and (38) to guarantee the existence of a stable fixed point in $w > 1/a$.

Now consider the map in $w < 1/a$. We aim to show that parameters can be chosen as shown in Figure 1(b), so that the two other branches of the map have a locally attracting invariant interval restricted to which there is a unique attracting set and positive Lyapunov exponents (actually, using standard techniques a great deal more could be said, but we will restrict attention here to the issue of multistability and discuss detailed dynamics elsewhere).

Let f denote the map (34). Then $f(0_-) = -1 < 0$ and $f(-1) = \gamma - 1$ which is in $w > 0$ provided $\gamma > 1$. Moreover, $f(0_+) = \gamma - 1$, so $f^2(0_-) = f(0_+)$, a consistency condition for grazing trajectories (two circuits with one sliding region and one graze of the sliding region can be viewed as two circuits with two slides or two circuits with one slide depending on how the grazing trajectory is interpreted). Since f is decreasing in $w < 0$, if $\gamma - 1 < 1/a$ and the map is decreasing in $0 < w < 1/a$ then the interval $[-1, \gamma - 1]$ will be invariant and there can be no stable periodic orbits if the slopes of both branches in this interval have magnitude larger than one. Thus the conditions required for the invariance of the interval $[-1, \gamma - 1]$ are

$$1 < \gamma < a^{-1} + 1, \quad \gamma a + b > 1 \tag{42}$$

together with the condition $f(\gamma - 1) > -1$, i.e.

$$-(\gamma a + b - 1)(\gamma - 1) + 1 > 0. \tag{43}$$

We now consider whether the inequalities (33), (36), (37), (38), (42) and (43) can be simultaneously satisfied.

Assume $\gamma > 1$. Then (37) is satisfied (a and b are positive), and we have the restriction $1 < \gamma < a^{-1} + 1$ of (42). For given a and γ the other constraints become

$$(\gamma - a)b < 1 + \gamma a^2, \quad (\gamma - a)b > -1 + \gamma a^2, \quad b > \frac{a+1}{\gamma} - a$$

from (36) and (38),

$$b > 1 - \gamma a, \quad b < 1 - \gamma a + \frac{1}{\gamma - 1}$$

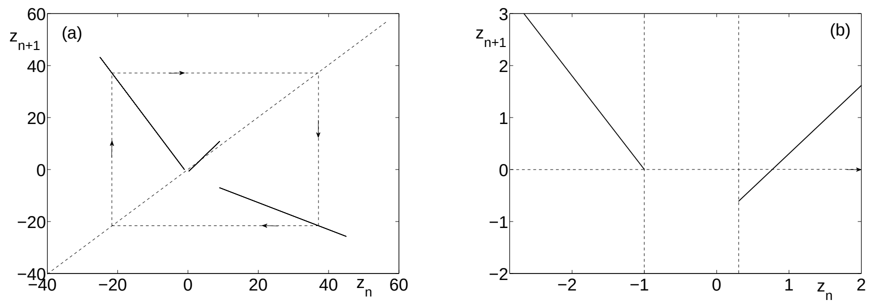

Figure 4: (a) A map $z_{n+1} = f(z_n)$ depicting the existence of stable period-three orbit coexisting with a fixed point without the sliding section for $a = -0.1$, $b = 0.7$, $\gamma = -C = 1.8$ and $\mu = 1$. (b) Zoom into a small segment ($z \in (-1,\ 0.3)$) of the $\{z = 0\}$-axis that is mapped onto the fixed point.

from (42) and (43), and of course $b > a^2$ from (33).

If $\gamma - a > 0$ ($1 < \gamma < (a+1)/a$, $a > 0$) and $m < M$, where

$$m = \max\left(\frac{-1+\gamma a^2}{\gamma - a}, a^2, \frac{a+1}{\gamma} - a, 1 - \gamma a\right) \tag{44}$$

and

$$M = \min\left(\frac{1+\gamma a^2}{\gamma - a}, 1 - \gamma a + \frac{1}{\gamma - 1}\right) \tag{45}$$

then for all $b \in (m, M)$ the complete set of inequalities will hold and the stable fixed point coexists with an attractor in $[-1, \gamma - 1]$ which we will show briefly is chaotic at the end of this section.

Now, by the same argument as in the previous section, $a < \dfrac{\gamma - 1}{\gamma^2 - \gamma + 1}$ implies that $m = 1 - \gamma a$, and since $1 - \gamma a$ is trivially less than the second term in the maximum of (45) the only constraint is

$$1 - \gamma a < \frac{1 + \gamma a^2}{\gamma - a}$$

which can be rewritten as $a > \dfrac{\gamma - 1}{\gamma^2 + 1}$ as in the statement of the Theorem.

Since $[-1, \gamma - 1]$ is compact it contains an attractor (possibly more than one though we do not believe so), and since the slope of the map has modulus greater than one at all points in the interval, the attractor is chaotic (all Lyapunov exponents are positive). Note that the interval $[-1, \gamma - 1]$ attracts an open neighbourhood $(-1 - \varepsilon, \gamma - 1 + \varepsilon)$ for $\varepsilon > 0$ sufficiently small (consider the second iterate of the map to see this).

4.3 Stable non-sliding orbit and period-three attractor

In this section we prove that another type of bistability is possible: there is a stable sliding periodic orbit, but that at the same time some initial conditions on the sliding surface are attracted to a stable periodic orbit which has no sliding section (this corresponds to the fixed point of the return map without sliding). In Fig. 4 we depict the results of iteration of the map (21) at $a = -0.1$, $b = 0.7$, $\gamma = -C = 1.8$ and $\mu = 1$. In the figure we can a segment of the z-axis which is not mapped onto itself. This shows that there is a set of points which never return to the switching manifold, and if the non-sliding orbit is stable then these points will be mapped into the fixed point (which is the case for the parameter values given above).

We have been unable to find an elegant proof of the existence of these regions, so to avoid unnecessary suffering on the part of the reader we provide the bare minimum required to demonstrate that such parameters exist. In particular we work with the fixed parameters

$$a = -0.1, \quad b = 0.7. \tag{46}$$

To show that solutions tend to the fixed point $X^* = (x^*, z^*)^T$ where

$$x^* = \frac{1}{1+b-a} \approx 0.5555, \quad z^* = -\frac{b}{1+b-a} \approx -0.3888 \tag{47}$$

we will need the following lemma.

Lemma 2 *Consider the map $F : \mathbb{R}^2 \to \mathbb{R}^2$ given by $F(x) = Ax + \begin{pmatrix} 1 \\ 0 \end{pmatrix}$ with A given by the linear part of the affine map (18) and parameters (46). Then*

$$|F(x) - F(y)| \leq 1.1|x - y| \tag{48}$$

and

$$|F^2(x) - F^2(y)| \leq 0.75|x - y| \tag{49}$$

for all $x, y \in \mathbb{R}^2$.

Proof: $|F(x) - F(y)|^2 = (x - y)^T A^T A(x - y)$ and direct calculation (with a little help from a computer) shows that the largest eigenvalue of $A^T A$ is a bit less than 1.02, and since $\sqrt{1.02} < 1.1$ the result holds.

Similarly $|F^2(x) - F^2(y)|^2 = (x - y)^T (A^2)^T A^2(x - y)$ and (again with help from a computer) the largest eigenvalue of $(A^2)^T A^2$ is a bit less than 0.52 and since $\sqrt{0.52} < 0.75$ the result holds.

This lemma will make it possible to show that some solutions on the line $x = 0$ tend to the fixed point of the return map in $x > 0$ without returning to $x < 0$. This, together with a calculation similar to that of previous subsections will be enough to demonstrate the following proposition.

Proposition 3 *If a and b are given by (46) then there exist some initial conditions $(0, z)$ such that the solution through $(0, z)$ remains in $x > 0$ and tends to the fixed point (47) (a periodic orbit for the flow); and the return map on $x = 0$ has a stable fixed point corresponding to an orbit which intersects the sliding surface twice in every three revolutions.*

The remainder of this section establishes this result.

Let us start with the existence of initial conditions on $x = 0$ which tend to the fixed point of the return map in $x > 0$. We consider a small line segment on $x = 0$ with $-1 < z < -1 + \epsilon$, with $0 < \epsilon \ll 1$, the end points of this line are $P = (0, -1)^T$, and $P_\epsilon = (0, -1 + \epsilon)^T$. By direct calculation $F(P) = (0, 0)$ and $F(P_\epsilon) = (\epsilon, 0)^T$, so the first iterate of the line segment lies in $x > 0$ close to the origin. Continuing:

$$F^2(P) = (1, 0)^T, \quad F^2(P_\epsilon) = F^2(P) + O(\epsilon)$$

and noting that for ϵ sufficiently small and positive, $F^k(P_\epsilon)$ is in $x > 0$ if $F^k(P)$ is in $x > 0$ we calculate

$$F^3(P) = (1 + a, -b)^T = (0.9, -0.7)^T$$

with $|F^3(P) - X^*| < 0.5$ (actually about 0.464). Hence $|F^4(P) - X^*| < 0.55$ and $|F^5(P) - X^*| < 0.375$ using the little lemma above. Now, since X^* is at least $x^* \approx 0.5555$ away from $x = 0$ induction on the lemma shows that the line segment remains in $x > 0$ for $\epsilon > 0$ small enough, and tends to the fixed point X^*.

The second part of the proposition follows from arguments very similar to those of the previous subsections. The return map on $z < -1$ is just

$$z' = C(z + 1)$$

or in coordinates $u = z + 1$,

$$u' = Cu + 1. \tag{50}$$

The second branch (points which miss the sliding surface on the first circuit, then hit at the second intersection), is defined if $a(z + 1) + 1 < 0$, i.e. $z > -1 + 1/|a|$ (as $a < 0$), and in coordinates $u = z + 1$ this becomes

$$u' = (Ca - b)u + C + 1, \quad u > 1/|a|. \tag{51}$$

Now fix

$$C = -1.8 \tag{52}$$

as in Figure 4, and note that the figure suggests the existence of a stable orbit of period two with one point in $u > 1/|a|$ and one point in $u < 0$. For the choice of parameters here the slope of the second map (51) is $Ca - b = -0.52$ and a period two orbit with one point on each branch is stable if $|C(Ca - b)| < 1$. Direct calculation shows $C(Ca - b) = 0.936$ so such an orbit, if it exists, is stable.

To verify existence note that if $u > 1/|a|$ then $u' = (Ca - b)u + C + 1 = -0.52u - 0.8 < 0$ and so using (50) there is a point of period two if

$$u = C(-0.52u - 0.8) + 1$$

or

$$u = u_2 = \frac{0.8C + 1}{1 - 0.936} = \frac{2.44}{0.064} = \frac{305}{8} = 38.125 \tag{53}$$

with its image in $u < 0$ being $u_2' = -20.635$. (Note that Figure 4 shows the solutions in $z-$coordinates, in which case the period two orbit is $\{-21.635, 37.125\}$.) This establishes the existence of a stable orbit of period two, corresponding to a solution of the differential equation that winds three times around the periodic orbit and intersects the sliding surface twice per period.

5 Conclusions

In the paper we study the occurrence of multistability triggered by the grazing-sliding bifurcation event. In particular, by considering a normal form for grazing-sliding bifurcations for 3-dimensional Filippov type flows, we reduce the investigations of system dynamics to that of one-dimensional maps. We prove that three different types of multistability can be encountered. Namely, two stable periodic orbits with segments of sliding, existing for the same value of the bifurcation parameter, can be born in the grazing-sliding bifurcation of a single stable orbit. Other unstable invariant sets may be involved in this bifurcations, but we are only interested in the attractors. The second scenario involving the birth of multiple attractors is that of the the chaotic attractor and a higher periodic orbit with sliding. Finally, a non-sliding and a sliding higher-periodic attractors may be born in the grazing sliding bifurcation. Again, also in these two latter scenarios, 'before' (or 'after') the bifurcation, only a single attractor exists locally around the grazing orbit. Numerical examples for every case are given.

This work suggests two different directions for future research. From a theoretical point of view it would be interesting to know how many different attractors can coexist close to grazing-sliding bifurcations, and to specify the sets of stable periodic orbits that can coexist. To understand the practical significance of multistability it would be useful to have explicit examples derived from applications that exhibit multistability.

6 Appendix

As we pointed out earlier different forms of the affine and PDM maps can be used for the numerical and analytical purposes. In particular, if we wish to compare the dynamics of a 3-dimensional Filippov type flow with that of the reduced map it is more natural to use the following transformations. We know that $\mu(b_1, b_2)^T = (I - A)(x^*, z^*)^T$ gives the information on the position of the fixed point of the affine map with respect to the switching surface, and it is convenient to use it as the bifurcation parameter. Letting $y_1 = x - x^*$ and $y_2 = z - z^*$ transforms P_A to

$$\begin{pmatrix} y_1 \\ y_2 \end{pmatrix} \mapsto A \begin{pmatrix} y_1 \\ y_2 \end{pmatrix} + A \begin{pmatrix} x^* \\ z^* \end{pmatrix} + (I - A) \begin{pmatrix} x^* \\ z^* \end{pmatrix} + \begin{pmatrix} x^* \\ z^* \end{pmatrix},$$

and we obtain a linear map of the form

$$\begin{pmatrix} y_1 \\ y_2 \end{pmatrix} \mapsto A \begin{pmatrix} y_1 \\ y_2 \end{pmatrix}. \tag{54}$$

The effect of the transformation on PDM is the inclusion of the parameter dependance; we have

$$\begin{pmatrix} y_1 \\ y_2 \end{pmatrix} \mapsto D \begin{pmatrix} y_1 \\ y_2 \end{pmatrix} + x^* \begin{pmatrix} -1 \\ C \end{pmatrix}, \tag{55}$$

where

$$D = \begin{pmatrix} 0 & 0 \\ C & 1 \end{pmatrix}. \tag{56}$$

Finally, assume $a_{12} \neq 0$ and let $[u, v]^T = L[y_1, y_2]^T$, where L is the transformation matrix (12). This leads to

$$P_A(u, v, \mu) = \begin{pmatrix} T & 1 \\ -D & 0 \end{pmatrix} \begin{pmatrix} u \\ v \end{pmatrix}, \tag{57}$$

and the discontinuity map PDM becomes

$$PDM(u, v, \mu) = \begin{pmatrix} 0 & 0 \\ C & 1 \end{pmatrix} \begin{pmatrix} u \\ v \end{pmatrix} + \begin{pmatrix} -1 \\ C \end{pmatrix} x^*. \tag{58}$$

Acknowledgments

Research partially funded by EPSRC grant EP/E050441/1, the University of Manchester and Manchester Metropolitan University.

References

[1] Y.Z. Tsypkin. *Relay Control Systems*. Cambridge University Press, Cambridge, U.K., 1984.

[2] R. C. Dorf and R. H. Bishop. *Modern control systems*. Aeeizh, 2002.

[3] W. M. van Spengen, R Puers, and I. De Wolf. A physical model to predict stiction in mems. *Journal of micromechanics and microengineering*, 12:702–713, 2002.

[4] H. de Jong. Modelling and simulations of genetic regulatory systems: A literature review. *Journal of computational biology*, 9(1):67–103, 2002.

[5] W. Chin, E. Ott, H. E. Nusse, and C. Grebogi. Grazing bifurcations in impact oscillators. *Physical Review E*, 50:4427–4444, 1994.

[6] L. E. Nusse and J. A. Yorke. Border collision bifurcation: an explanation for observed bifurcation phenomena. *Physical Review E*, 49:1073–1076, 1994.

[7] H. Dankowicz and A. B. Nordmark. On the origin and bifurcations of stick-slip oscillations. *Physica D*, 136:280–302, 1999.

[8] S. Banerjee and C. Grebogi. Border collision bifurcations in two-dimensional piecewise smooth maps. *Physical Review E*, 59:4052–4061, 1999.

[9] M. H. Fredriksson and A. B. Nordmark. On normal form calculations in impact oscillators. *Proceedings of the Royal Society London A*, 456:315–329, 2000.

[10] A. P. Ivanov. Stabilization of an impact oscillator near grazing incidence owing to resonance. *Journal of Sound and Vibration*, 162:562–565, 1993.

[11] F. Dercole, A. Gragnani, Yu. A. Kuznetsov, and S. Rinaldi. Numerical sliding bifurcation analysis: An application to a relay control system. *IEEE Trans. Circuits Systems I Fund. Theory Appl.*, 50:1058–1063, 2003.

[12] R. I. Leine and H. Nijmeijer. *Dynamics and Bifurcations of Non-Smooth Mechanical Systems*, volume 18. Springer - Verlag, 2004.

[13] J. Sieber. Dynamics of delayed relay systems. *Nonlinearity*, 19:2489–2527, 2006.

[14] M. di Bernardo, C. Budd, A.R. Champneys, and P. Kowalczyk. *Piecewise-smooth Dynamical Systems — Theory and Applications*, volume 163 of *Applied Mathematical Sciences*. Springer-Verlag, 2008.

[15] M. Dutta, H. E. Nusse, E. Ott, J. A. Yorke, and G. Yuan. Multiple attractor bifurcations: A source of unpredictability in pieceiwse smooth systems. *Physical Review Letters*, 83(21):4281–4281, 1999.

[16] A. B. Nordmark and P. Kowalczyk. A codimension-two scenario of sliding solutions in grazing-sliding bifurcations. *Nonlinearity*, 19:1–26, 2006.